EPJ Web of Conferences **96**, 01005 (2015)
DOI: 10.1051/epjconf/20159601005

Heavy Quarkonia at LHCb

R. Cardinale[1,a] on behalf of the LHCb collaboration.

[1] *Department of Physics and INFN Genova, via Dodecaneso 33, 16146 Genova (Italy)*

Abstract. The pp collision data collected by the LHCb experiment during Run I provides a great opportunity for heavy flavour studies. The latest results on exotic states and quarkonia production are reported.

1 Introduction

Thanks to the large center-of-mass energy available at the LHC, $b\bar{b}$ and $c\bar{c}$ pairs are produced with great abundancy, which provides great opportunities for studying production and properties of heavy hadrons. The LHCb experiment has collected data in 2011 and 2012 corresponding to an integrated luminosity of $1\,\text{fb}^{-1}$ at $\sqrt{s} = 7\,\text{TeV}$ centre-of-mass energy and $2\,\text{fb}^{-1}$ at $\sqrt{s} = 8\,\text{TeV}$ respectively. With this large statistics, its efficient trigger, its excellent momentum resolution and particle identification, LHCb is the ideal place to perform hadron spectroscopy studies.

2 Exotic states

In the last few years a number of quarkonium-like states, generally called as X, Y and Z that do not fit the conventional picture, have been discovered. The existence of tetraquarks, hadronic molecules, and other bound states involving gluons has been invoked to explain these exotic states, but a compelling unified description has not yet emerged. At LHCb high-precision studies of the $X(3872)$ and the $Z(4430)^-$ states have been performed.

2.1 X(3872)

The $X(3872)$, discovered by Belle in 2003 in the $J/\psi\pi^+\pi^-$ invariant mass distribution of $B^- \to J/\psi\pi^+\pi^-K^+$ decays [1] and subsequently observed by several other experiments, was the first charmonium-like state found not to fit the conventional quarkonium description. The $X(3872)$ is particularly intriguing since decaying into $J/\psi\pi^+\pi^-$ leads to a natural interpretation as a charmonium excitation, on the other hand the closeness of its mass to the $D^{*0}\bar{D}^0$ threshold and its prominent decay to $D^{*0}\bar{D}^0$ suggest that it may be an example of a hadron molecule with an extremely small binding energy. After measuring the $X(3872)$ mass and production cross-section in pp collisions [2], LHCb has also determined its quantum numbers to be $J^{PC} = 1^{++}$ [3] ruling out with a significance of more than eight standard deviations the only alternative assignment allowed by previous measurements $J^{PC} = 2^{-+}$ [4]. These quantum numbers favour the conventional charmonium state $\chi_{c1}(2P)$. Despite this large experimental effort, after more than 10 years since its discovery, nowadays its nature is still unclear.

One of the quantities, which is sensitive to the nature of the $X(3872)$ state is the ratio of the branching fractions for radiative decays to $\psi(2S)\gamma$ and $J/\psi\gamma$

$$R_\psi = \frac{\mathcal{B}(X(3872) \to \psi(2S)\gamma)}{\mathcal{B}(X(3872) \to J/\psi\gamma)}$$

This ratio is predicted to be in the range $(3-4)\times10^{-3}$ for a $D^{*0}\bar{D}^0$ molecule [7], 1.2-15 for a pure $c\bar{c}$ state [5, 6] and 0.5-5 for a molecule-charmonium mixture [8]. The BaBar collaboration has measured a relative large branching fraction for the $X(3872) \to \psi(2S)\gamma$ decay, with $R_\psi = 3.4 \pm 1.4$ [9], a result generally inconsistent with a pure molecular interpretation; in contrast, no significant signal was found by Belle [10]. At LHCb, a search for the $X(3872)$ into $\psi(2S)\gamma$ is performed using $B^+ \to X(3872)K^+$ decays and reconstructing the $\psi(2S)$ meson in $\mu^+\mu^-$ channel [11]. The data sample corresponds to the full statistics recorded by LHCb during Run1, i.e. $1\,\text{fb}^{-1}$ at $\sqrt{s} = 7\,\text{TeV}$ and $2\,\text{fb}^{-1}$ at $\sqrt{s} = 8\,\text{TeV}$.

The signal yield is determined from a two-dimensional unbinned maximum likelihood fit in the $(J\psi\gamma K^+, J/\psi\gamma)$ and $(\psi(2S)\gamma K^+, \psi(2S)\gamma)$ invariant masses. The invariant mass distributions of $\psi\gamma$ and $\psi\gamma K^+$ combinations for the J/ψ and $\psi(2S)$ channels are shown in Figure 1. The observed signal in the $\psi(2S)$ channel of 36.4 ± 9.0 events has a significance of 4.4. Using the measured yields, the ratio of the branching fractions is calculated to be

$$R_\psi = 2.46 \pm 0.63(stat) \pm 0.29(syst)$$

This value agrees with the expectations both for a pure charmonium and a molecular-charmonium mixture but does not support a pure $D\bar{D}^*$ molecular interpretation.

[a] e-mail: roberta.cardinale@ge.infn.it

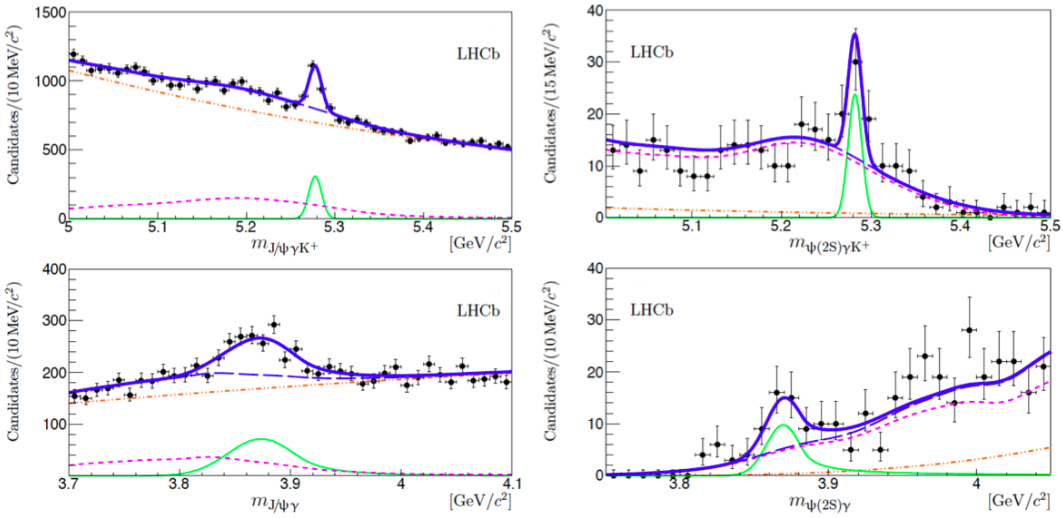

Figure 1. (Top) On the left (right) the distribution of the $J/\psi\gamma K^+$ ($\psi(2S)\gamma K^+$) invariant mass with fit projection overlaid, restricted to those candidates with $J/\psi\gamma$ ($\psi(2S)\gamma$) invariant mass within $\pm 3\sigma$ from the $X(3872)$ peak position. (Bottom) On the left (right) distribution of the $J/\psi\gamma$ ($\psi(2S)\gamma$) invariant mass with fit projection overlaid, restricted to those candidates with $J/\psi\gamma K^+$ ($\psi(2S)\gamma K^+$) invariant mass within $\pm 3\sigma$ from the B^+ peak position. The total fit (thick solid blue) together with the signal (thin solid green) and background components (dash-dotted orange for the combinatorial, dashed magenta for the peaking component and long dashed blue for their sum) are shown.

2.2 $Z(4430)^-$

The exotic state that attracts a lot of attention recently is the charged charmonium-like $Z(4430)^-$. For a charged charmonium state, the $Z(4430)^-$ has a minimum quark content of $c\bar{c}du$ which clearly does not fit into the traditional quark model. This state was first observed by the Belle collaboration as a charged resonance structure in the $\psi(2S)\pi^-$ invariant mass distribution of the $B^0 \to \psi(2S)K^-\pi^+$ decays [12]. Subsequent reanalysis of the data was performed with 2D and 4D amplitude analyses [13]. BaBar collaboration analysed the same decays using a model independent approach and it concluded that the enhancement could be explained as a reflection of the know K^* states but did not rule out the existence of the $Z(4430)^-$ either [14].

The LHCb collaboration has investigated resonant structures in $B^0 \to \psi(2S)K^+\pi^-$ decays, with the $\psi(2S)$ decaying into two muons, using pp collision data corresponding to an integrated luminosity of 3 fb^{-1} [15]. About 25000 B^0 candidates were reconstructed with approximately 4% of background in the signal region, as shown in Figure 2. The sample size is about 10 times larger than the ones analysed by B-factories. Dalitz plot of the selected events in the signal region is shown in Figure 3. Clear contributions from $K^*(892)$ and kaon states around 1.43 GeV are visible as two vertical bands. The $Z(4430)^+$ state would correspond to the horizontal band at $m^2(\psi(2S)\pi^-) \sim 20\,\text{GeV}^2$.

LHCb has performed an analysis based on the model-independent approach developed by BaBar to check whether the $m_{\psi(2S)\pi^-}$ spectrum can be understood in terms of any combination of known K^* resonances. No constraint is imposed on these resonances besides restricting

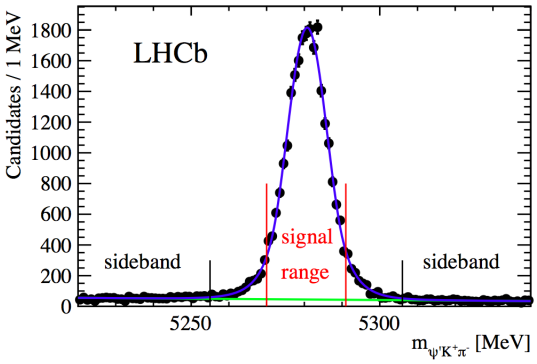

Figure 2. Invariant mass distribution for $B^0 \to \psi(2S)K^+\pi^-$ decay candidates. In the invariant mass distribution the fit (blue line) with a double-sided Crystal Ball signal shape and linear background (green line) are superimposed to the data points.

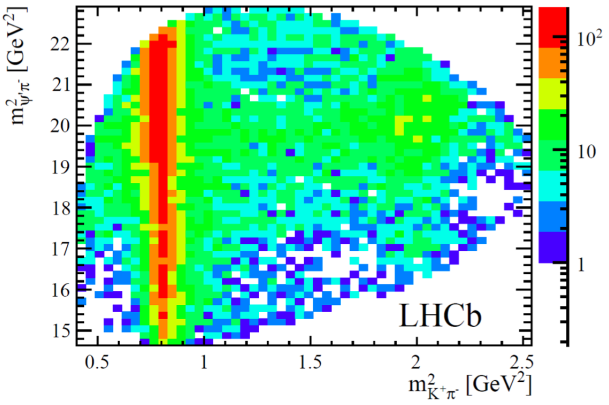

Figure 3. Dalitz plot for $B^0 \to \psi(2S)K^+\pi^-$ decay candidates.

their maximal spin to two, as the $K^+\pi^-$ invariant mass spectrum is dominated by S, P and D partial waves. The description of the $K^+\pi^-$ angular structure is performed in terms of Legendre polynomial moments. The analysis shows that the relatively narrow peaking structure in $m_{\psi(2S)\pi^-}$ cannot be described in terms of moments of K^* resonances as shown in Figure 4.

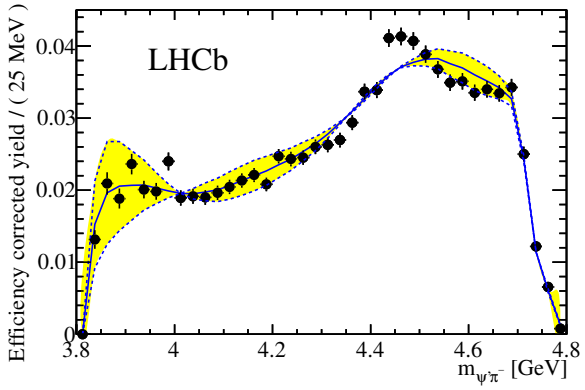

Figure 4. Background-subtracted and efficiency-corrected $m_{\psi(2S)\pi^-}$ distribution superimposed with the expected distribution of Legendre polynomial moments and their correlated statistical uncertainty (yellow band).

A full amplitude fit was performed to be able to extract quantitative information about the $Z(4430)^-$ such as its mass, width and spin. The amplitude was calculated in a four-dimensional space using the invariant masses $m^2_{K^+\pi^-}$ and $m^2_{\psi(2S)\pi^-}$, the $\cos\theta_{\psi(2S)}$ which is the $\psi(2S)$ helicity angle and the ϕ angle between the K^{*0} and the $\psi(2S)$ planes in the B^0 rest frame.

The amplitude model includes all known K^{*0} resonances in various spin states with nominal mass at or slightly above kinematic limits. As shown in Figure 5, the data are not well described when considering only known $K^* \to K^+\pi^-$ resonances, while a better description is obtained when including in the fit a $Z(4430)^- \to \psi(2S)\pi^-$ with $J^P = 1^+$. Other J^P hypothesis ($0^-, 1^-, 2^+$ and 2^-) are ruled out with a significance larger than nine standard deviations, thus confirming previous indications from Belle [16]. The fit gives for the mass and the width of the $Z(4430)^-$

$$M_{Z^-} = 4475 \pm 7\,\text{MeV},$$

$$\Gamma_{Z^-} = 172 \pm 13\,\text{MeV}$$

and for the amplitude fraction

$$f_{Z^-} = (5.9 \pm 0.9)\%.$$

which are consistent with Belle results [16]. Uncertainties are statisical only. The significance of the $Z(4430)^-$ contribution is 13.9σ. An additional fit is performed where the $Z(4430)^-$ amplitude is represented as a combination of independent complex amplitudes ($\text{Re}\,A^{Z(4430)^-}$, $\text{Im}A^{Z(4430)^-}$) at six equidistant points in the $m^2_{\psi(2S)\pi^-}$ range to address the question if the $Z(4430)^-$ is a real bound state that follows a resonant behaviour. The resulting Argand diagram,

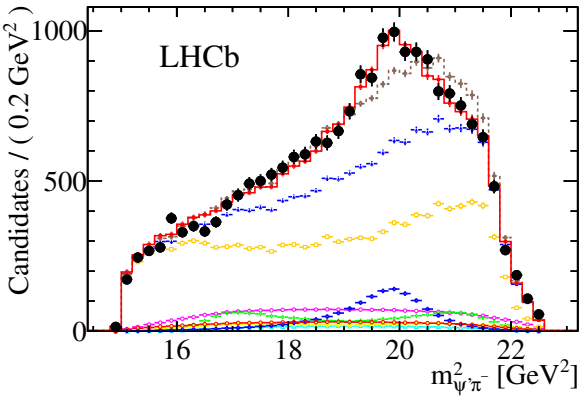

Figure 5. Projection of the data and of the 4D amplitude fit onto the $m^2_{\psi(2S)\pi^-}$ axis.

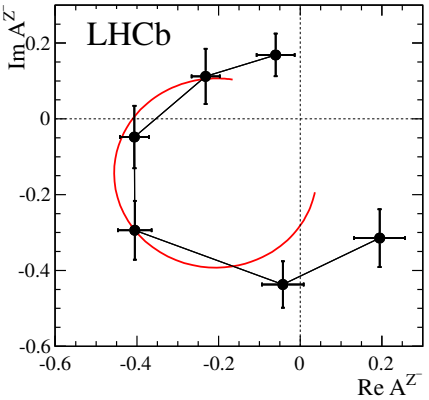

Figure 6. Argand diagram for the fitted binned $Z(4430)^-$ amplitude. The Breit-Wigner evolution with the mass and width from the nominal fit is shown as a red curve.

shown in Figure 6, exhibits a quasi circular pattern, which is consistent with a rapid phase transition at the peak of the amplitude, just as expected for a resonance, providing a strong argument in favour of the resonant character of the $Z(4430)^-$ state.

3 Heavy quarkonia production

Measurements of heavy quarkonia production is fundamental to test QCD models. The mechanism for the production of quarkonia in hadronic collisions is in fact not yet completely understood. It is well known that the LO Colour Singlet Model leads to predictions of the cross-sections which are in disagreement with the observations at high p_T. New theoretical approaches have been proposed in recent years. The debate is still open and experimental confirmations from the LHC experiments are needed to determine the reliability of the proposed models. Unique measurements of the production of quarkonia and quarkonia-like states in the forward rapidity range ($2 < y < 4.5$) and in the low p_T range have been performed at LHCb.

3.1 χ_b production

Feed-down contributions from P-wave quarkonium state to S-wave quarkonium states might be of crucial importance for the comparison between experimental results and theory prediction for prompt production of S-wave quarkonia. It can also impact on the interpretation of the measured polarization of S-wave vector quarkonia. Moreover measurements of the relative production rates of P-wave to S-wave quarkonia (and tensor-to-vector ratios) can provide valuable information on colour-octet matrix elements [17–19]. Two different analyses which study the χ_b production in LHCb and measure the fraction of $\Upsilon(nS)$ originating from χ_b decays have been performed, one using calorimetric photons [20], the other one using photons converted in the detector material [21].

The first analysis uses prompt muon pairs selected requiring for each muon a p_T larger than 1 GeV. Further cuts refine the quality and the purity of the muons. Cuts improving the two-prong common vertex and the compatibility of this vertex with the primary vertex are applied. Three very clean peaks, $\Upsilon(1S)$, $\Upsilon(2S)$ and $\Upsilon(3S)$, are observed in the $m_{\mu^+\mu^-}$ mass distribution as shown in Figure 7. Photons reconstructed using the calorimeter are

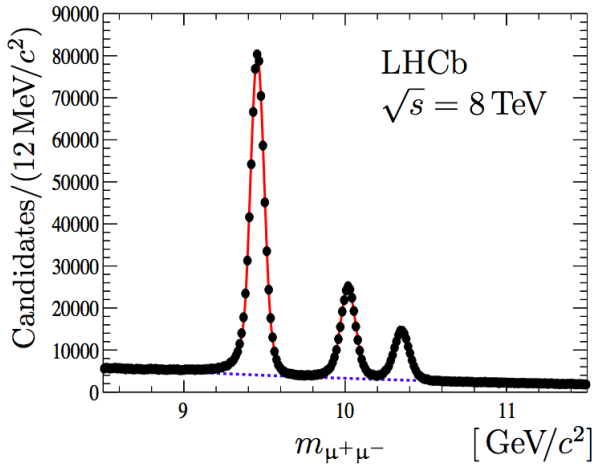

Figure 7. Invariant mass distribution for selected dimuon candidates.

combined to each muon pair having an invariant mass within 150 MeV of one of the Υ states to form a χ_b. The χ_b yields are determined from an extended maximum likelihood fit. The fit model consists of the sum of signal components for all kinematically allowed $\chi_b(mP) \to \Upsilon(nS)\gamma$ decays and combinatorial background (see Figure 8). In the fit, the χ_{b0} contribution of the multiplet is neglected while the χ_{b1} and the χ_{b2} are fitted simultaneously assuming a fixed mass difference, Δm_{12} and a fixed ratio of yields. This assumption is needed since the χ_b mass resolution does not allow to separate these two states. The assumption on the relative χ_{b1}/χ_{b2} contribution and the electromagnetic calorimeter energy scale are entering as the dominant systematic errors on the measurement of the $\chi_b(3P)$ mass. This mass is measured to be

$$m_{\chi_{b1}(3P)} = 10511.3 \pm 1.7(stat) \pm 2.4(syst)\,\mathrm{MeV}/c^2.$$

The feed-down fractions $R^{\chi_b(mP)}_{\Upsilon(nS)}$ of Υ originating from radiative χ_b decays are determined by calculating the ratio of the Υ and the χ_b yields in each p_T^Υ bin and for each decay $\chi_b(mP) \to \Upsilon(nS)\gamma$ with $m > n$. In this ratio, most of the systematic errors cancel. The remaining systematic errors are dominated by the uncertainties related to the photon reconstruction at low p_T and the various assumptions made in the χ_b mass fit: χ_{b1}/χ_{b2} ratio, p_T dependence on the mass fits and modelling of the mass resolution. The results of the feed-down fractions , for each Υ state as a function of their p_T are shown in the three plots of Figure 9. A big fraction of $\Upsilon(nS)$ production originates from radiative decays of $\chi_b(mP)$ states. The large value of this fraction impacts on the interpretation of experimental data on Υ production and polarization. When data on Υ production and polarization are compared with theory predictions, as well as when different theory predictions are compared among themselves, it is often implicitly assumed that the fraction of $\Upsilon(3S)$ mesons produced by feed down from higher states is small. The large measured value of $R^{\chi_l b}_{\Upsilon(3S)}(3P)$ indicates that these $\Upsilon(3S)$ assumptions need to be revisited.

The measurement of the relative rate of $\chi_{b1}(1P)$ and $\chi_{b2}(1P)$ production has been performed using $\Upsilon(1S)\gamma$ and $\Upsilon(2S)\gamma$ decays using photons that converted to e^+e^- pairs in the detector [21]. In addition the analysis performed a measurement of the $\chi_b(3P)$ mass. Measurements of the relative rate of $J = 1$ and $J = 2$ states provide information on the colour octet contribution. This relative rate is also predicted to have the same dependence on the meson transverse momentum in χ_b and χ_c states, once the p_T of the χ_b meson is scaled by the ratio of χ_c and χ_b masses. The kinematically allowed transitions $\chi_b(1P) \to \Upsilon(1S)\gamma$, $\chi_b(2P) \to \Upsilon(1S)\gamma$, $\chi_b(3P) \to \Upsilon(1S)\gamma$ and $\chi_b(3P) \to \Upsilon(2S)\gamma$ are studied. The Υ meson is reconstructed in the dimuon final state and only photons that convert in the detector material are used. The converted photons are reconstructed using e^+ and e^- tracks, allowing separation of the χ_{b1} and χ_{b2} peaks, due to the improved energy resolution of converted photons with respect to that of photons identified with the calorimeter. The ratio of the χ_{b2} to χ_{b1} production cross-sections is measured in three p_T^Υ ranges from 5 to 25 GeV/c in the rapidity range $2.0 < y < 4.5$. Figure 10 shows a comparison of the measured valued with LO NRQCD predictions. The measurement obtained by LHCb for the χ_c production ratio with the p_T axis scaled accordingly is also shown for comparison. The χ_b results are in good agreement with the scaled $\chi_c$results. These results are not precise enough to establish the deviation from unity predicted by theory at low p_T, but the agreement is better with a flat dependence. In addition the measurement of the $m(\chi_b(3P))$ and of the mass splitting Δm_{12} between $J = 1$ and $J = 2$ states has been performed. The results for the $\chi_b(1, 2P)$ mass splittings

$$\Delta m_{12}(1P) = 19.81 \pm 0.65(stat) \pm 0.20(syst)\,\mathrm{MeV}/c^2$$
$$\Delta m_{12}(2P) = 12.3 \pm 2.6(stat) \pm 0.6(syst)\,\mathrm{MeV}/c^2$$

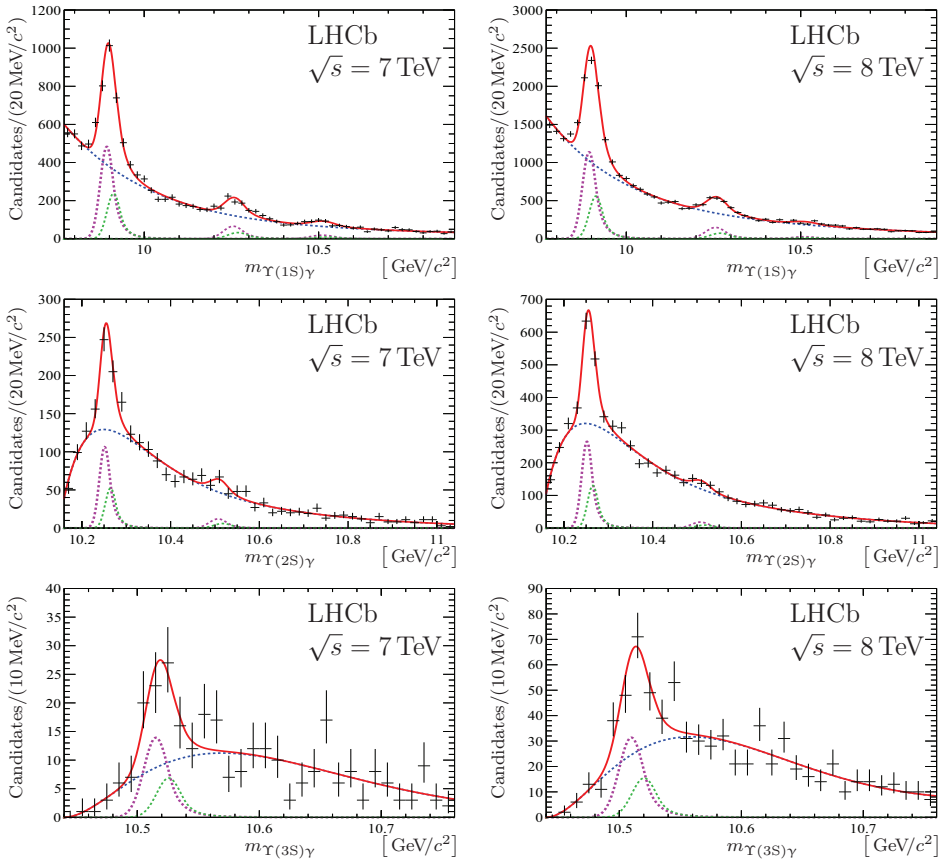

Figure 8. Distributions of the corrected mass $m_{\Upsilon(nS)\gamma}$ for the selected χ_b candidates (black points) decaying into (top row) $\Upsilon(1S)$, (middle row) $\Upsilon(2S)$ and (bottom row) $\Upsilon(3S)$, in the transverse momentum ranges given in the text, for (left) $\sqrt{s} = 7$ TeV and (right) 8 TeV data. Each plot shows also the result of the fit (solid red curve), including the background (dotted blue curve) and the signal (dashed green and magenta curves) contributions. The green dashed curve corresponds to the χ_{b1} signal and the magenta dashed curve to the χ_{b2} signal.

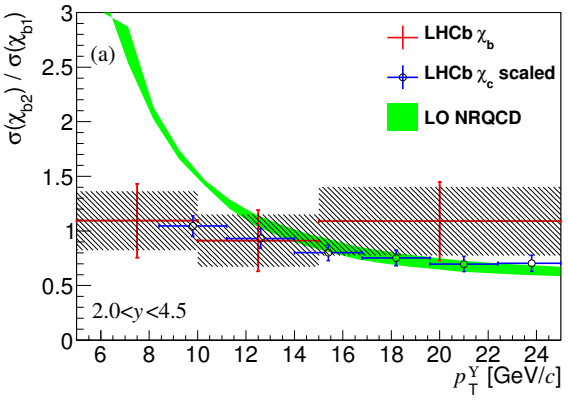

Figure 10. Relative production cross-sections of χ_{b1} and χ_{b2} mesons as a function of p_T^Υ. The plot shows the comparison of this measurement (the hatched rectangles show the statistical uncertainties and the red crosses the total experimental uncertainty) to the LO NRQCD prediction (green band) [18], and to the LHCb χ_c result (blue crosses) [24], where the p_T axis has been scaled by $m(\chi_b)/m(\chi_c) = 2.8$.

are in agreement with the world average values. The mass for the $\chi_{b1}(3P)$ is measured to be

$$m(\chi_{b1}(3P)) = 10515.7^{+2.2}_{-3.9}(stat)^{+1.5}_{-2.1}(syst)\,\mathrm{MeV/c^2}$$

This result is compatible with the measurement performed by LHCb with the radiative decays to the $\Upsilon(3S)$ meson that uses non-converted photons. A combined value of the two measurements is

$$m(\chi_{b1}(3P)) = 10512.1 \pm 2.1(exp) \pm 0.9(model)\,\mathrm{MeV/c^2}$$

where the experimental systematic uncertainties are uncorrelated since the photon reconstruction is based on different subdetectors, while the uncertainty related to the model used for summing the $J = 1$ and $J = 2$ contributions are fully correlated. These results are compatible with ATLAS [22] and D0 [23] measurements.

3.2 $\eta_c(1S)$ production cross-section

The investigation of the lowest state, the $\eta_c(1S)$ meson, can provide important additional information on the long-distance matrix elements. In particular, the heavy-quark

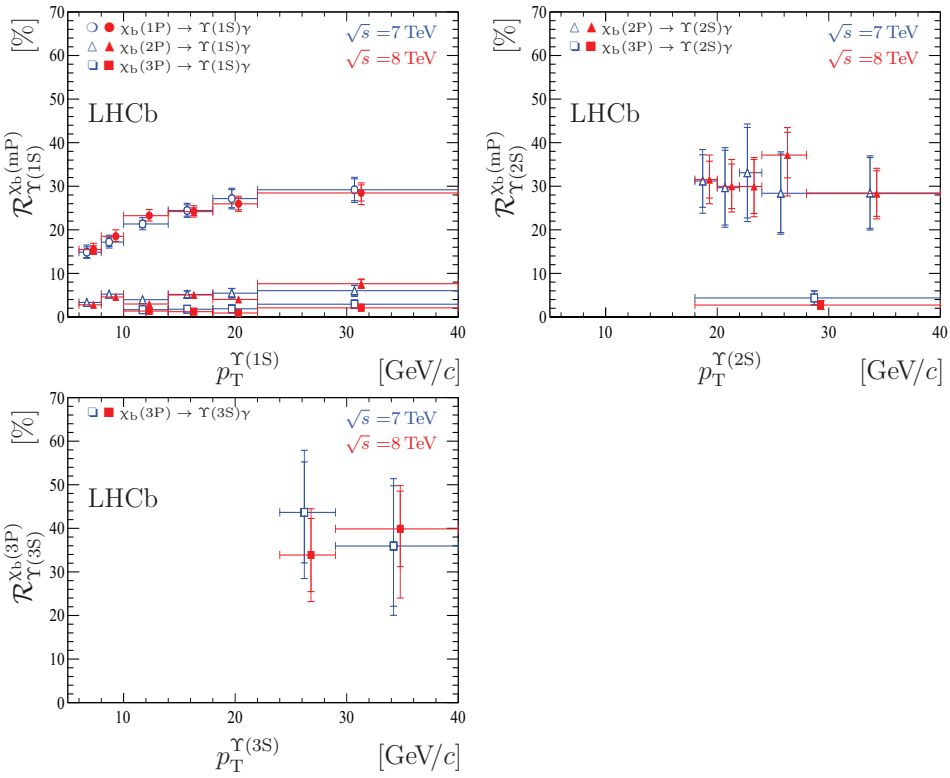

Figure 9. Feed-down fractions $R^{\chi_b(mP)}_{\Upsilon(nS)}$ as a function of p_T^{Υ}. Open (solid) symbols correspond to data collected at $\sqrt{s}$ = 7(8) TeV respectively. Inner error bars represent statistical uncertainties while outer error bars represent the sum in quadrature of statistical and systematic uncertainties.

spin-symmetry relation between the $\eta_c(1S)$ and J/ψ matrix elements can be tested [25, 26], with the NLO calculations predicting a different dependence of the production rates on charmonium transverse momentum, p_T, for spin singlet ($\eta_c(1S)$) and triplet (J/ψ, χ_{cJ}) states. Thus, a measurement of the p_T dependence of the $\eta_c(1S)$ production rate can have important implications. LHCb has performed the first measurement of the cross-section for the prompt production of $\eta_c(1S)$ mesons in pp collisions at $\sqrt{s}$ = 7 TeV and $\sqrt{s}$ = 8 TeV centre-of-mass energies, as well as the b-hadron inclusive branching fraction into $\eta_c(1S)$ final states. The measurements have been performed relative to the J/ψ channel which allows partial cancellation of systematic uncertainties in the ratio.

The signal selection is largely performed at the trigger level. The offline analysis, in addition, requires the transverse momentum of the protons to be $p_T > 2.0\,\text{GeV/c}$ and restricts charmonium candidates to the rapidity range $2.0 < y < 4.5$. Prompt and b-decays candidates are separated using the pseudo-decay time. The invariant mass for selected prompt candidates is reported in Figure 11. The cross-section for prompt production of $\eta_c(1S)$ relative to the prompt J/ψ production has been measured in the rapidity range $2.0 < y < 4.5$ and in the transverse-momentum range $p_T > 6.5\,\text{GeV/c}$ to be at $\sqrt{s} = 7\,\text{TeV}$

$$\sigma_{\eta_c(1S)}/\sigma_{J/\psi} = 1.74 \pm 0.29 \pm 0.28 \pm 0.18_{\mathcal{B}}$$

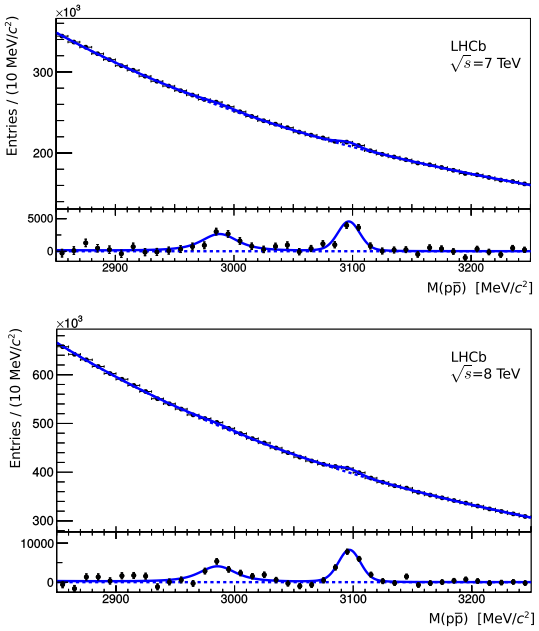

Figure 11. $p\bar{p}$ invariant masses for prompt candidates (upper panel in each plot) and distribution of differences between data and the background distribution resulting from the fit (lower panel in each plot) in data at a) $\sqrt{s}$ = 7 TeV and b) $\sqrt{s}$ = 8 TeV centre-of-mass energies.

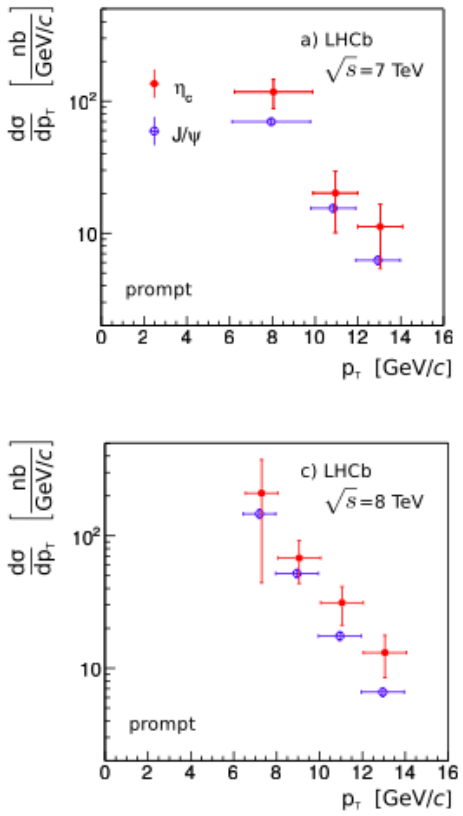

Figure 12. Prompt production spectra as a function of transverse momentum for $\eta_c(1S)$ mesons (red filled circles). The p_T spectra of J/ψ from Refs. are shown for comparison as blue open circles.

and at $\sqrt{s} = 8\,\text{TeV}$

$$\sigma_{\eta_c(1S)}/\sigma_{J/\psi} = 1.60 \pm 0.29 \pm 0.25 \pm 0.17_{\mathcal{B}}$$

where the uncertainties are statistical, systematic and that on the ratio of branching fractions of the $\eta_c(1S)$ and J/ψ decays to $p\bar{p}$ final states. This is the first measurement of η_c production at an hadron machine. The cross-section for the $\eta_c(1S)$ prompt production is in agreement with the colour-singlet leading order calculations, while the predicted cross-section exceeds the observed value by two orders of magnitude when the colour-octet LO contribution is taken into account. However the NLO contribution is expected to significantly modify the LO result [28].

The $\eta_c(1S)$ differential cross-section as a function of p_T is obtained by fitting the $p\bar{p}$ invariant mass spectrum in three or four bins of p_T (see Figure 12). The p_T dependencies of the $\eta_c(1S)$ and J/ψ production rates exhibit similar behaviour in the kinematic region studied.

The inclusive branching fraction of b-hadron decays into $\eta_c(1S)$ mesons with $p_T > 6.5\,\text{GeV/c}$, relative to the corresponding fraction into J/ψ mesons, is measured, for the first time, to be

$$\mathcal{B}(b \to \eta_c(1S)X)/\mathcal{B}(b \to J/\psi X) = \\ = 0.421 \pm 0.055 \pm 0.022 \pm 0.045_{\mathcal{B}}$$

4 Conclusions

LHCb has used the large data sample available to perform studies of exotic charmonium-like states. After having determined the $X(3872)$ quantum numbers [3], the decay $X(3872) \to \psi(2S)\gamma$ has been observed with a significance of 4.4σ [11]. This result favours the interpretation of the $X(3872)$ as a mixture of a $D^{*0}\bar{D}^0$ molecule and charmonium. LHCb also provided confirmation of the $Z(4430)^-$ state seen by Belle and it established its spin-parity to be 1^+ [15]. From study of the phase motion the resonance character of this state has been demonstrated.

Moreover unique measurements of the production of quarkonia have been obtained with the LHCb experiment. These studies provide valuable input to improve the accuracy of theoretical models. All these results demonstrate the excellent performance of the LHCb experiment and the excellent prospects for hadronic spectroscopy.

References

[1] S. K. Choi *et al.* [Belle Collaboration], Phys. Rev. Lett. **91** (2003) 262001 [hep-ex/0309032].
[2] R. Aaij *et al.* [LHCb Collaboration], Eur. Phys. J. C **72** (2012) 1972 [arXiv:1112.5310 [hep-ex]].
[3] R. Aaij *et al.* [LHCb Collaboration], Phys. Rev. Lett. **110** (2013) 222001 [arXiv:1302.6269 [hep-ex]].
[4] A. Abulencia *et al.* [CDF Collaboration], Phys. Rev. Lett. **98** (2007) 132002 [hep-ex/0612053].
[5] B. Q. Li and K. T. Chao, Phys. Rev. D **79** (2009) 094004 [arXiv:0903.5506 [hep-ph]].
[6] A. M. Badalian, V. D. Orlovsky, Y. A. Simonov and B. L. G. Bakker, Phys. Rev. D **85** (2012) 114002 [arXiv:1202.4882 [hep-ph]].
[7] J. Ferretti, G. Galatà and E. Santopinto, Phys. Rev. D **90** (2014) 5, 054010 [arXiv:1401.4431 [nucl-th]].
[8] E. J. Eichten, K. Lane and C. Quigg, Phys. Rev. D **73** (2006) 014014 [Erratum-ibid. D **73** (2006) 079903] [hep-ph/0511179].
[9] B. Aubert *et al.* [BaBar Collaboration], Phys. Rev. Lett. **102** (2009) 132001 [arXiv:0809.0042 [hep-ex]].
[10] V. Bhardwaj *et al.* [Belle Collaboration], Phys. Rev. Lett. **107** (2011) 091803 [arXiv:1105.0177 [hep-ex]].
[11] R. Aaij *et al.* [LHCb Collaboration], Nucl. Phys. B **886** (2014) 665 [arXiv:1404.0275 [hep-ex]].
[12] S. K. Choi *et al.* [BELLE Collaboration], Phys. Rev. Lett. **100** (2008) 142001 [arXiv:0708.1790 [hep-ex]].
[13] R. Mizuk *et al.* [BELLE Collaboration], Phys. Rev. D **80** (2009) 031104 [arXiv:0905.2869 [hep-ex]].
[14] B. Aubert *et al.* [BaBar Collaboration], Phys. Rev. D **79** (2009) 112001 [arXiv:0811.0564 [hep-ex]].
[15] R. Aaij *et al.* [LHCb Collaboration], Phys. Rev. Lett. **112** (2014) 22, 222002 [arXiv:1404.1903 [hep-ex]].
[16] K. Chilikin *et al.* [Belle Collaboration], Phys. Rev. D **88** (2013) 074026 [arXiv:1306.4894 [hep-ex]].
[17] Y. Q. Ma, K. Wang and K. T. Chao, Phys. Rev. D **83** (2011) 111503 [arXiv:1002.3987 [hep-ph]].

[18] A. K. Likhoded, A. V. Luchinsky and S. V. Poslavsky, Phys. Rev. D **86** (2012) 074027 [arXiv:1203.4893 [hep-ph]].

[19] A. K. Likhoded, A. V. Luchinsky and S. V. Poslavsky, arXiv:1305.2389 [hep-ph].

[20] R. Aaij *et al.* [LHCb Collaboration], Eur. Phys. J. C **74** (2014) 10, 3092 [arXiv:1407.7734 [hep-ex]].

[21] R. Aaij *et al.* [LHCb Collaboration], JHEP **1410** (2014) 88 [arXiv:1409.1408 [hep-ex]].

[22] G. Aad *et al.* [ATLAS Collaboration], Phys. Rev. Lett. **108** (2012) 152001 [arXiv:1112.5154 [hep-ex]].

[23] V. M. Abazov *et al.* [D0 Collaboration], Phys. Rev. D **86** (2012) 031103 [arXiv:1203.6034 [hep-ex]].

[24] R. Aaij *et al.* [LHCb Collaboration], JHEP **1310** (2013) 115 [arXiv:1307.4285 [hep-ex]].

[25] M. Butenschoen and B. A. Kniehl, Phys. Rev. Lett. **108** (2012) 172002 [arXiv:1201.1872 [hep-ph]].

[26] K. T. Chao, Y. Q. Ma, H. S. Shao, K. Wang and Y. J. Zhang, Phys. Rev. Lett. **108** (2012) 242004 [arXiv:1201.2675 [hep-ph]].

[27] S. S. Biswal and K. Sridhar, J. Phys. G **39** (2012) 015008 [arXiv:1007.5163 [hep-ph]].

[28] F. Maltoni and A. D. Polosa, Phys. Rev. D **70** (2004) 054014 [hep-ph/0405082].